Multi-objective Optimization for Upper Body Posture Prediction

Jingzhou Yang[*], R. Timothy Marler[†], HyungJoo Kim[‡], Jasbir S. Arora[§], and Karim Abdel-Malek[**]

Virtual Soldier Research Program, Center for Computer-Aided Design, The University of Iowa, 111 Engineering Research Facility, Iowa City, IA 52242-1000

The demand for realistic autonomous virtual humans is increasing, with potential application to prototype design and analysis for a reduction in design cycle time and cost. In addition, virtual humans that function independently, without input from a user or a database of animations, provide a convenient tool for biomechanical studies. However, development of such avatars is limited. In this paper, we capitalize on the advantages of optimization-based posture prediction for virtual humans. We extend this approach by incorporating multi-objective optimization (MOO) in two capacities. First, the objective sum and lexicographic approaches for MOO are used to develop new human performance measures that govern how an avatar moves. Each measure is based on a different concept with different potential applications. Secondly, the objective sum, the min-max, and the global criterion methods are used as different means to combine these performance measures. It is found that although using MOO to combine the performance measures generally provides reasonable results especially with a target point located behind the avatar, there is no significant difference between the results obtained with different MOO methods.

Nomenclature

$\mathbf{q}$	=	generalized coordinates (joint angles)
$\mathbf{q}^N$	=	neutral position
$\mathbf{x}(\mathbf{q})$	=	position vector of the end-effector
$\mathbf{f}(\mathbf{q})$	=	vector of objective functions
$f_i(\mathbf{q})$	=	objective function (human performance measure)
F	=	aggregate objective function
$g_i(\mathbf{q})$	=	inequality constraints
$h_i(\mathbf{q})$	=	equality constraints
DOF	=	number of degrees of freedom
$\mathbf{w}$	=	vector of joint-displacement weights
$\boldsymbol{\gamma}$	=	vector of discomfort weights
λ	=	min-max parameter

[*] Research Engineer, Center for Computer Aided Design, Tel: +001-319-353-2249, jyang@engineering.uiowa.edu.
[†] PhD Candidate, Department of Mechanical and Industrial Engineering.
[‡] Post Doctoral Fellow, Center for Computer Aided Design.
[§] Professor, Department of Civil and Environmental Engineering, AIAA Senior Member.
[**] Associate Professor, Department of Biomedical Engineering.

I. Introduction

THE development and use of virtual humans (computer simulations of humans) have recently gained momentum for engineering product design and biomechanical studies. In terms of engineering, it is well recognized that computer-based simulations and prototypes can save time and money. However, actual human interaction plays a key role in prototype development, and although virtual prototypes have been used extensively in the design and manufacturing processes, virtual humans that interact with such prototypes have not yet been leveraged thoroughly. Thus, avatars that act effectively as real humans can provide a key element in engineering design and analysis. In terms of biomechanics, understanding posture and musculoskeletal motion is critical in the analysis of joints and extremities. To this end, virtual humans can provide a convenient and reliable means for studying movement and musculoskeletal functions.

Most of the methods for modeling human posture and motion take one of the following approaches. One may use *classical animation* based on either experimental data or user-manipulation of avatars. However, this approach lacks autonomy; a separate picture or animation must be created for each posture and/or motion. In fact, we distinguish between animation and *simulation*, suggesting that virtual humans should be simulations that inherently and independently demonstrate movements, reactions, and decision-making capabilities, which appear natural and appropriate given any general scenario. Another approach for modeling humans involves *inverse kinematics*, which entails solving a system of equations to determine parameters for the human model that define position and motion. However, this approach can be prohibitively slow, especially with a larger number of degrees of freedom (DOF). Recently, an *optimization-based* approach has surfaced. This approach entails optimizing objective functions that represent human performance measures, such as joint displacement, discomfort, etc. These performance measures govern how the avatar moves. This approach ensures autonomous movement regardless of the scenario. In addition, it can be implemented in real time.

Despite its advantages, development of the optimization-based approach is in its infancy, used primarily with robotics. Consequently, it has only been applied to systems with relatively few degrees of freedom, although it can provide computationally efficient models of more complex potentially redundant systems such as human skeletons. In addition, the advantages of multi-objective optimization (MOO) have not yet been exploited. Thus, we use MOO in two capacities: 1) the development of new human performance measures and 2) the combination of different measures to model more accurately, how humans move. In order to aggregate multiple measures, we propose a MOO-based approach for posture prediction. Integrating the disciplines of multi-objective optimization and human modeling yields exciting results for both fields.

A. Literature Review

Although there is ample literature concerning motion prediction for humans and robots, there is limited material concerning human posture prediction. Most currently available methods are limited in terms of the autonomy they afford the avatar and in terms of the complexity of the human models that are used. In addition, the use of optimization-based posture prediction is also limited, and the use of multi-objective optimization (for the development of human performance measures or for posture prediction) has not yet been addressed.

Most classical animation involves empirical-statistical modeling using anthropometrical data. These data are collected either from thousands of experiments with human subjects, or from simulations with three-dimensional computer-aided human-modeling software (Porter *et al* 1990; Das and Singupta 1995). The data are then analyzed statistically in order to form predictive posture models. These models have been implemented in simulation software along with various methods for selecting the most probable posture given a specific scenario (Beck and Chaffin 1992; Zhang and Chaffin 1996; Das and Behara 1998; Faraway *et al* 1999). Although this approach is based on actual human data and thus need not be verified in terms of realism, it involves a time-consuming data collection process often requiring thousands of human subjects.

The inverse kinematics approach to posture prediction, which uses biomechanics and kinematics as predictive tools, has received substantial attention. With this approach, the position of a limb is modeled mathematically with the goal of formulating a set of equations that provide the joint variables (Jung *et al* 1992; 1995; Kee *et al* 1994; Jung and Choe 1996; Wang 1999; Tolani *et al* 2000). However, as suggested earlier, this approach is restricted to relatively simple models.

In the field of robotics, predicting a "posture" is not a consideration. However, it is important to predict the path of a point on a robotic arm. To this end, considerable research has been conducted with optimization-based path planning of robot manipulators with minimum traveling-time as a cost function to predict the path of a manipulator (Lin *et al* 1983, Shin and Mckay 1986, Chen 1991). Some authors consider multi-objective optimization but only in so much as they simply add two different objective functions. Weights may be used in a weighted sum, but the weights serve only as scaling factors; there is no indication of preference between the two objectives. MOO is not thoroughly exploited in terms of potential methods or in terms of theoretical analysis of the results. For instance, Zhao and Bai (1999) propose a optimization approach with load or torque as an objective, and they use multi-objective optimization to combine these objectives. Saramago and Steffen J. (1998, 2000) present a multi-objective optimization solution to the problem of moving a robot manipulator. They optimize the traveling time and minimize the mechanical energy of the actuators, considering dynamics and collision avoidance of moving obstacles. Saramago and Ceccarelli (2002) proposed a similar multi-objective optimization approach with payload constraints. Because much of the focus for motion prediction has been on robotics, little work has been conducted with the development of objective functions that are tailored to human posture.

Abdel-Malek *et al* (2001b, 2001c) study single-objective optimization-based human posture prediction using genetic algorithms, and Mi *et al* (2001) extend this work to real-time simulation. However, no other work concerning optimization-based human posture prediction has been conducted, and no work concerning multi-objective optimization with posture prediction is available.

B. Overview of the Paper

Based on the above-mentioned deficiencies in the current state of the art, we pursue the following objectives in this paper:

1) Incorporate MOO in optimization-based posture prediction algorithms;
2) Using MOO, develop new human performance measures that more accurately simulate how humans move;
3) Compare the performance of basic MOO methods;
4) Evaluate the concept of basing human motion on multiple performance measures simultaneously.

Before providing a brief review of key concepts associated with MOO, we present an overview of the human modeling method that is necessary for the analysis. Next, the general optimization formulation used for posture prediction is discussed, various human performance measure are explained, and the MOO methods for combining these measures are summarized. Visual and numerical results are shown, first by using each human performance measure independently, and then by combining them with MOO. These methods are compared in terms of their computational performance and in terms of the realism of the consequent postures.

II. Overview of Virtual Human Model

Essentially, the human body is modeled as a kinematic system, a series of links connected by revolute joints that represent musculoskeletal joints such as the wrist, elbow, or shoulder. Our approach entails finding the rotational displacement of these joints necessary to optimize one or more objective functions that represent human performance measures. In this section, the fundamentals of the kinematic model are presented.

In order to represent gross motion, a basic model for the upper body is developed that incorporates the torso, spine, shoulders, and arms. The rotation of each joint in the human body is represented by a generalized coordinate q_i, as shown for the series of links in Figure 1.

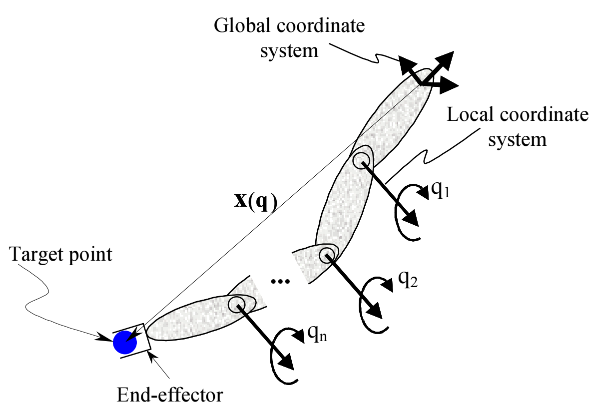

Figure 1. General Kinematic Model.

Each generalized coordinate is associated with a local coordinate system. $\mathbf{q} \in \mathbf{R}^n$ is the vector of n generalized coordinates in an n-DOF model and represents a specific posture. $\mathbf{x}(\mathbf{q}) \in R^3$ is the position vector in Cartesian space that describes the location of the *end-effector* as a function of the generalized coordinates, with respect to the global coordinate system. Thus, the position of the end-effector is defined as follows:

$$\mathbf{x}(\mathbf{q}) = \begin{bmatrix} x(\mathbf{q}) \\ y(\mathbf{q}) \\ z(\mathbf{q}) \end{bmatrix} \tag{1}$$

An end-effector is the end-point in a series of links such as an arm. We are concerned with finding the values of the generalized coordinates when the position of the end-effector is constrained with respect to the global coordinate system.

The Denavit-Hartenberg (DH) method (Denavit and Hartenberg, 1955) is used to determine **x** for a given **q**. The DH-method provides a matrix notation and approach for relating the position of a point in one coordinate system to another coordinate system, by using a unique transformation matrix. Such an approach is useful with kinematic systems in which a series of components are connected by joints. A local coordinate system and a local transformation matrix are associated with each joint, describing its configuration with respect to the previous joint and coordinate system. Multiple transformation matrices can be combined to determine the position of any point on the kinematic system with respect to any local coordinate system or with respect to a global coordinate system, based on all of the joint displacements. This approach has been used for modeling human biomechanics, kinematics, and dynamics (Jung *et al,* 1995; Abdel-Malek *et al*, 2001a; Yang *et al*, 2003). In this report, the DH-method is used to describe a series of links that lead from the waist of a human model to the upper extremities. Details concerning the method are given by Marler (2004).

With this study, a 21-DOF model for the human torso and right arm is used, as shown in Figure 2.

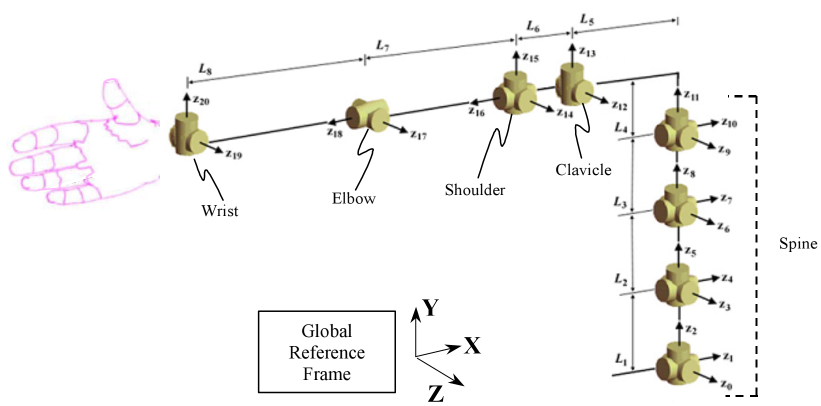

Figure 2. 21-DOF Kinematic Model.

The distances between the joints are represented by L_i, and the axes of rotation are indicated by z_i where z_i corresponds to q_{i+1}. q_1 through q_{12} represent the spine. q_{13} through q_{17} represent the shoulder and clavicle. q_{18} through q_{21} represent the right arm. The end-effector is the tip of the index finger, and the set of points that can be contacted by the end-effector is called the *reach envelope*. The details of this model are provided by Farrell and Marler (2004).

Although this study focuses on upper-body posture prediction, Figure 2 represents just one part of a complete virtual human model called Santos, which is illustrated in Figure 3.

III. Overview of Multi-Objective Optimization

In this section, the fundamentals of multi-objective optimization are reviewed. The general MOO problem is posed as follows:

$$
\begin{aligned}
&\text{Find: } \mathbf{q} \in R^{DOF} \\
&\text{to minimize: } \mathbf{f}(\mathbf{q}) = \begin{bmatrix} f_1(\mathbf{q}) & f_2(\mathbf{q}) & \cdots & f_k(\mathbf{q}) \end{bmatrix}^T \\
&\text{subject to: } g_i(\mathbf{q}) \le 0 \quad i = 1, 2, \cdots, m \\
&\qquad\qquad\quad h_j(\mathbf{q}) = 0 \quad j = 1, 2, \cdots, e
\end{aligned}
\tag{2}
$$

where k is the number of objective functions, m is the number of inequality constraints, and e is the number of equality constraints. $\mathbf{q} \in E^{DOF}$ is a vector of design variables. $\mathbf{f}(\mathbf{q}) \in E^k$ is a vector of objective functions $f_i(\mathbf{q}) : E^{DOF} \to E^1$. The *feasible design space* is defined as $\mathbf{\Pi} = \{\mathbf{q} \,|\, g_j(\mathbf{q}) \le 0,\ j = 1, 2, ..., m;$ and $h_i(\mathbf{q}) = 0,\ i = 1, 2, ..., e\}$. The *feasible criterion space* is defined as $\mathbf{Z} = \{\mathbf{f} \in R^k \text{ such that } \mathbf{f} = \mathbf{f}(\mathbf{q}), \mathbf{q} \in \mathbf{\Pi}\}$. Points in the feasible criterion space that can be determined using a specific method are called *attainable*. The point in the criterion space where all of the objectives have a minimum value simultaneously is called the *utopia point* $\mathbf{f}^{\circ}$. In general, $\mathbf{f}^{\circ}$ is unattainable; it rarely is possible to fully optimize each individual objective function independently and simultaneously, whether the problem is constrained or not.

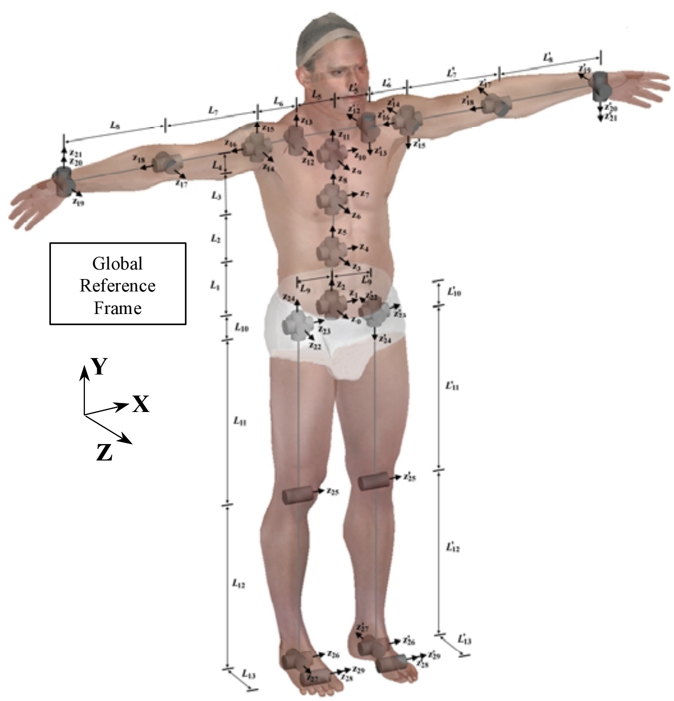

Figure 3. Santos, a Complete Virtual Human.

The idea of a solution for (2), where multiple objectives may conflict with one another (e.g., what minimizes one function may increase another), can be unclear. Consequently, the idea of *Pareto optimality* is used to describe solutions for MOO problems. A solution point is Pareto optimal if it is not possible to move from that point and improve at least one objective function without detriment to any other objective function. Based on this definition, the minimum of a single objective function is Pareto optimal if it is unique. Alternatively, a point is *weakly Pareto optimal* if it is not possible to move from that point and improve all objective functions simultaneously.

Typically, there are infinitely many Pareto optimal solutions for a MOO problem. Thus, it is often necessary to incorporate user preferences in order to determine or select a single suitable solution. With methods that incorporate *a priori articulation of preferences*, the user indicates the relative importance of the objective functions or desired goals before running the optimization algorithm. Different methods allow one to articulate preferences in different ways, but the most common approach is to have the user set parameters such as weights. Alternatively, preferences may not be available, the decision-maker may not know or cannot concretely define what he/she prefers, or the problem may be purely mathematical. Thus, some methods involve *no articulation of preferences*. Although the exact solution point provided by such methods is somewhat arbitrary, these types of methods can provide useful benchmark results for multi-objective analysis.

IV. Multi-objective Posture Prediction

In this section, we formulate the posture prediction optimization problem. In doing so, MOO is used in two capacities. First, it is used to develop new human performance measures. It is then used to combine these measures, which serve as multiple objective functions, in a final optimization problem. Details concerning the methods discussed in this section are given by Marler and Arora (2004), whereas brief overviews of the methods are given throughout this section.

A. Design Variables and Constraints

As suggested earlier, the design variables for the final MOO problem are the generalized coordinates q_i, which indicate the rotation of the joints in units of degrees. The vector **q** represents the consequent posture.

The first constraint, called the *distance* constraint, requires the end-effector to contact the target point. In addition, each generalized coordinate is constrained to lie within predetermined limits. q_i^U represents the upper limit for q_i, and q_i^L represents the lower limit. These limits ensure that the virtual human does not assume a position that is completely unrealistic given the nature of actual human joints.

B. Human Performance Measures

1. Joint Displacement

The first performance measure represents joint displacement; it is based on the *weighted sum method* for multi-objective optimization. This method always provides a Pareto optimal solution and entails minimizing the following aggregate objective function:

$$F = \sum_{i=1}^{k} w_i f_i(\mathbf{q}) \tag{3}$$

where w_i are positive weights used for a priori articulation of preferences. In general, they indicate the relative importance of the objective functions. The value of each weight is only significant relative to the other weights and relative to the value of its corresponding objective function.

The details of the joint displacement function are explained as follows. Let q_i^N be the *neutral position* of a joint measured from the starting *home configuration*. The home configuration is characterized by $\mathbf{q} = \mathbf{0}$, and the neutral position $\mathbf{q}^N$ represents a relatively comfortable position. Then, conceptually, the displacement from the neutral position for a particular joint is given by $\left|q_i - q_i^N\right|$. However, to avoid numerical difficulties and non-differentiability, the terms $(q_i - q_i^N)^2$ are used. Each of these 21 terms (one for each degree of freedom) can be treated as an individual objective function, which are combined using a weighted sum. Because some joints tend to be activated more than others, the scalar weights w_i are introduced to stress the importance of particular joints. The cumulative joint displacement is modeled using the following weighted sum:

$$f_{Joint\ displacement}(\mathbf{q}) = \sum_{i=1}^{DOF} w_i \left(q_i - q_i^N\right)^2 \tag{4}$$

The values for the weights are given in Table 1.

Table 1: Joint Weights for Joint-Displacement.

Joint Variable	Joint Weight	Comments
q_1, q_4, q_7, q_{10}	100	Used with both positive and negative values of $q_i - q_i^N$
q_2, q_5, q_8, q_{11}	100 1000	When $q_i - q_i^N > 0$ When $q_i - q_i^N < 0$
q_3, q_6, q_9, q_{12}	5	Used with both positive and negative values of $q_i - q_i^N$
q_{13}	75	Used with both positive and negative values of $q_i - q_i^N$
q_{14}, q_{15}, q_{16}	1	Used with both positive and negative values of $q_i - q_i^N$
q_{17}	50 1	When $q_i - q_i^N > 0$ When $q_i - q_i^N < 0$
$q_{18}, q_{19}, q_{20}, q_{21}$	1	Used with both positive and negative values of $q_i - q_i^N$

For this model, the neutral position is chosen based on observation of the skinned model in Figure 3 rather than a skeletal model like the one shown in Figure 2. The resulting vector $\mathbf{q}^N$ is defined as

$$q_i^N = 0;\ i = 1,\ldots,12,19,20 \tag{5}$$
$$q_{13}^N = -15.0,\ q_{14}^N = 20.0,\ q_{15}^N = 100.0,\ q_{16}^N = -10.0,\ q_{17}^N = -80.0,\ q_{18}^N = -35.0,\ q_{21}^N = 15.0$$

This generally represents a posture with the arms straight down, parallel to the torso. With the joint displacement performance measure, the avatar's position gravitates towards the neutral position.

2. Delta-Potential-Energy

In this section, we discuss a potential-energy function, which is indirectly based on the weighted sum method for MOO. However, in this case, the weights are based on the mass of different segments of the body. With the previous function, the weights are set based on intuition and experimentation, and although the postures obtained by minimizing joint displacement are realistic, there are other ways to assign relative importance to the components of the human performance measure. The idea of potential energy provides one such alternative.

We represent the primary segments of the upper body with six lumped masses: three for the lower, middle, and upper torso, respectively; one for the upper arm; one for the forearm; and one for the hand. We then determine the potential energy for each mass. The heights of these masses, rather than the joint displacements for the generalized coordinates, provide the components of the human performance measure. Mathematically, the weight (force of gravity) of a segment of the upper body provides a multiplier for movement of that segment in the vertical direction. The height of each segment is a function of generalized coordinates, so, in a sense, the weights of the lumped masses replace the scalar multipliers, w_i, which are used in the joint displacement function.

If the potential energy function were used directly, there would always be a tendency to bend over, thus reducing potential energy. Consequently, we actually minimize the *change* in potential energy. Each link in a segmented serial chain, as depicted in Figure 4 (e.g., the forearm), has a specified center of mass.

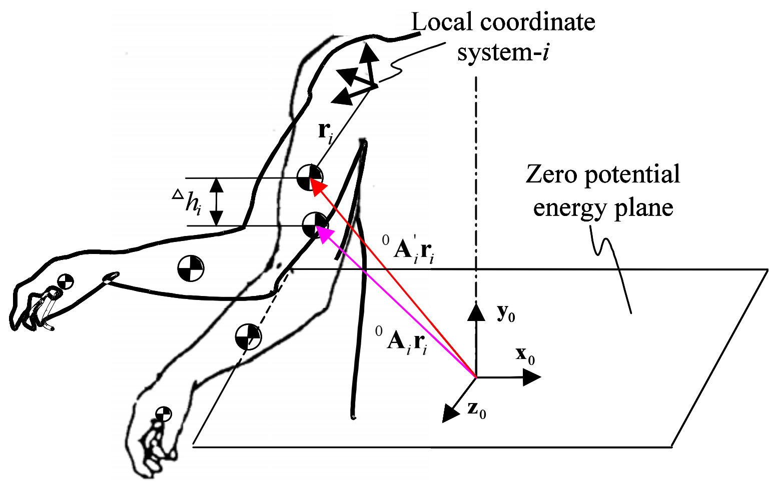

Figure 4. Illustration of the Potential Energy of the Upper Body.

The vector from the origin of a link's local coordinate system to its center of mass is given by ${}^i\mathbf{r}_i$, where the subscript indicates the relevant local coordinate system. In order to determine the position and orientation of any part of the body, we use the transformation matrices ${}^{(i-1)}A_i$, which are 4×4 matrices that relate local coordinate system-i to local coordinate system-$i-1$. Consequently, $\mathbf{r}_i$ is actually an augmented 4×1 vector with respect to local coordinate system i, rather than a 3×1 vector typically used with Cartesian space. $\mathbf{g}=\begin{bmatrix}0 & -g & 0 & 0\end{bmatrix}^T$ is the augmented gravity vector. When the human upper body moves from one configuration to another, there are two potential energies, $P_i^{'}$ which is associated with the initial configuration and P_i which is associated with the current configuration. Therefore, for the first body part in the chain (the lower torso), the potential energies are $P_1^{'}=m_1\mathbf{g}^T\,{}^0\mathbf{A}_1^{'}\mathbf{r}_1$ and $P_1=m_1\mathbf{g}^T\,{}^0\mathbf{A}_1\mathbf{r}_1$. The potential energies for the second body part are $P_2^{'}=m_2\mathbf{g}^T\,{}^0\mathbf{A}_1^{'}\,{}^1\mathbf{A}_2^{'}\mathbf{r}_2$ and $P_2=m_2\mathbf{g}^T\,{}^0\mathbf{A}_1\,{}^1\mathbf{A}_2\mathbf{r}_2$. The potential energies for the i^{th} body part are $P_i^{'}=m_i\mathbf{g}^T\,{}^0\mathbf{A}_1^{'}\cdots{}^{i-1}\mathbf{A}_i^{'}\mathbf{r}_i$ and $P_i=m_i\mathbf{g}^T\,{}^0\mathbf{A}_1\cdots{}^{i-1}\mathbf{A}_i\mathbf{r}_i$. In Figure 4, $\triangle h_i$ is the y-component of the vector ${}^0\mathbf{A}_1^{'}\cdots{}^{i-1}\mathbf{A}_i^{'}\mathbf{r}_i-{}^0\mathbf{A}_1\cdots{}^{i-1}\mathbf{A}_i\mathbf{r}_i$. The final objective function, which is minimized, is defined as follows:

$$f_{Delta-potential-energy}(\mathbf{q})=\sum_{i=1}^{\kappa}\left(P_i-P_i^{'}\right)^2 \qquad (6)$$

Note that (6) can be written in the form of a weighted sum as follows:

$$f_{Delta-potential-energy}(\mathbf{q})=\sum_{i=1}^{\kappa}\left(m_i g\right)^2\left(\Delta h_i\right)^2 \qquad (7)$$

where $\left(m_i g\right)^2$ represent the weights and $\left(\Delta h_i\right)^2$ act as the individual objective functions, $\kappa=6$ is the number of lumped masses. In this case, the initial position is the neutral position describe in relation to joint displacement. With this performance measure, the avatar again gravitates towards the neutral position. However, horizontal motion of the lumped masses has no affect on the objective function.

3. *Discomfort*

The discomfort human-performance-measure is based on the *lexicographic method* for MOO. A priori articulation of preferences is used with this method, as it was with the weighted sum, but preferences are articulated in a slightly different format. Rather than assign weights that indicate relative importance, one simply prioritizes the objectives. Then, one objective at a time is minimized in a sequence of separate optimization problems. After an objective has been minimized, it is incorporated as a constraint in the subsequent problems. The solution to this method is Pareto optimal, if it is unique.

The concept behind this new discomfort measure is that groups of joints are utilized sequentially. That is, in an effort to reach a particular target point, one first uses one's arm. Then, if necessary, one bends the torso. Finally, if the target is still out of reach, one may extend the clavicle joint. The lexicographic method for MOO is designed to incorporate this type of preference structure. However, solving a sequence of optimization problems can be time consuming and impractical for real-time applications such as human simulation. The weighted sum method can be used to approximate results of the lexicographic method if the weights have infinitely different orders of magnitude (Miettinen, 1999; Romero, 2000). This results in the weights shown in Table 2.

Table 2: Joint Weights for Discomfort.

Joint Variable	Joint Weight	Comments
$q_1,\ldots,q_{12}$	1×10^4	Used with both positive and negative values of $q_i - q_i^N$
q_{13},q_{14}	1×10^8	Used with both positive and negative values of $q_i - q_i^N$
$q_{15},\ldots,q_{21}$	1	Used with both positive and negative values of $q_i - q_i^N$

Although weights are used here, they do not need to be determined as indicators of the relative significance of their respective joints; they are simply fixed mathematical parameters. In addition, the exact values of the weights are irrelevant; they simply have to have significantly different orders of magnitude. Note that some of the weights in Table 1 (used with joint displacement) are discontinuous, and this is because movement in various directions can result in different degrees of acceptability. These discontinuities can lead to computational difficulties. However, with this discomfort objective, such discontinuities are avoided.

The weights in Table 2 are used in a function that is based on (4) with the neutral position defined as shown in (5). However, prior to applying the weights, each term in (4) is normalized as follows:

$$\Delta q^{norm} = \frac{q_i - q_i^N}{q_i^U - q_i^L} \tag{8}$$

With this normalization scheme, each term $\left(\Delta q_i^{norm}\right)^2$ acts as an individual objective function and has values between zero and one.

Generally, this approach works well but often results in postures with joints extended to their limits, and such postures can be uncomfortable. To rectify this problem, extra terms are added to the discomfort function such that the discomfort increases significantly as joint values approach their limits. The final discomfort function is given as follows:

$$f_{Discomfort}(\mathbf{q}) = \frac{1}{G}\sum_{i=1}^{DOF}\left[\gamma_i\left(\Delta q_i^{norm}\right) + G\times QU_i + G\times QL_i\right] \tag{9}$$

$$QU_i = \left(0.5Sin\left(\frac{5.0\left(q_i^U - q_i\right)}{q_i^U - q_i^L} + 1.571\right) + 1\right)^{100}$$

$$QL_i = \left(0.5Sin\left(\frac{5.0\left(q_i - q_i^L\right)}{q_i^U - q_i^L} + 1.571\right) + 1\right)^{100}$$

where $G\times QU$ is a penalty term associated with joint values that approach their upper limits, and $G\times QL$ is a penalty term associated with joint values that approach their lower limits. γ_i are the weights defined in Table 2. Each term varies between zero and G, as $\left(q_i^U - q_i\right)/\left(q_i^U - q_i^L\right)$ and $\left(q_i - q_i^L\right)/\left(q_i^U - q_i^L\right)$ vary between zero and one. Figure 5 illustrates the curve for the following function, which represents the basic structure of the penalty terms:

$$Q = \left(0.5Sin\left(5.0r + 1.571\right) + 1\right)^{100} \tag{10}$$

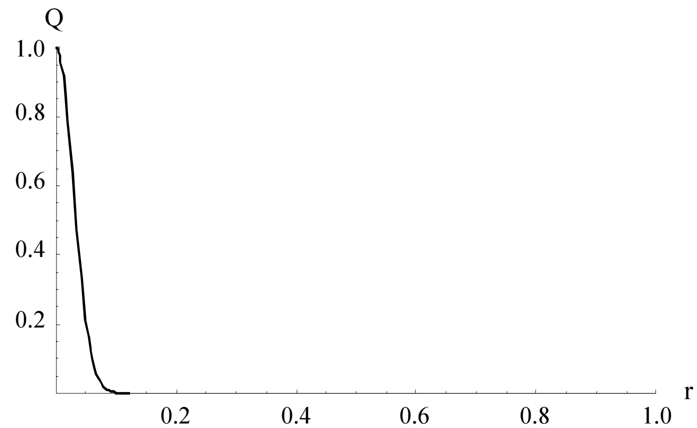

Figure 5. Graph of Discomfort Joint-Limit Penalty Term.

r represents either $\left(q_i^U - q_i\right)/\left(q_i^U - q_i^L\right)$ or $\left(q_i - q_i^L\right)/\left(q_i^U - q_i^L\right)$. Thus, as Figure 5 illustrates, the penalty term has a value of zero until the joint value reaches the upper or lower 10% of its range, where either $\left(q_i^U - q_i\right)/\left(q_i^U - q_i^L\right) \le 0.1$ or $\left(q_i - q_i^L\right)/\left(q_i^U - q_i^L\right) \le 0.1$. The curve for the penalty term is differentiable, and reaches its maximum of $G = 1\times10^6$ when $x = 0$. The final function in (9) is multiplied by $1/G$ to avoid extremely high function-values.

C. Posture Prediction Formulation

Given the above-mentioned design variables, constraints, and human performance measures, the optimum posture for the 21-DOF system shown in Figure 2 is determined by solving the following MOO problem:

$$\begin{aligned}
&\text{Find: } \mathbf{q} \in R^{DOF} \\
&\text{to minimize: } \textit{Joint displacement}, \textit{Delta-potential-energy}, \text{ and } \textit{Discomfort} \\
&\text{subject to: } distance = \left\| \mathbf{x}\left(\mathbf{q}\right)^{end\text{-}effector} - \mathbf{x}^{target\ point} \right\| \le \varepsilon \\
&\qquad q_i^L \le q_i \le q_i^U;\ i = 1,2,\ldots,DOF
\end{aligned} \tag{11}$$

where ε is a small number that approximates zero. All optimization problems are solved using the software SNOPT (Gill *et al*, 2002), which uses sequential quadratic programming (Arora, 2004).

After solving (11) by using each performance measure independently (with single-objective optimization), we use three different approaches to MOO. Each of these methods involves no articulation of preferences. This is because the intent here is simply to investigate the advantages and/or disadvantages of incorporating multiple human performance measures simultaneously. While there are many different approaches for MOO with no articulation of preferences (Marler and Arora, 2004), we consider fundamental methods that tend to be less demanding computationally and lend themselves well to real-time simulations.

First, we consider the objective sum method, which simply involves using (3) with all of the weights set to one. Then, we use the *min-max method* with which one minimizes the following function:

$$F = \max_{1\le i\le k} f_i$$

(12)

Because (12) can involve potential discontinuities, it is reformulated with an additional design variable λ and additional constraints, as follows:

$$\begin{aligned}&\text{Find: } \lambda, \mathbf{q} \\ &\text{to minimize: } \lambda \\ &\text{subject to: } f_i(\mathbf{q}) - \lambda \le 0; \quad i = 1,2,3\end{aligned} \tag{13}$$

We refer to the additional constraints as *function-constraints*. Although the min-max method may yield non-Pareto optimal solutions in some cases, it always provides weakly Pareto-optimal solutions. Finally, the *global criterion method* is used, with which the following aggregate function is minimized:

$$F = \left[\sum_{i=1}^{k} (f_i)^p\right]^{1/p} \tag{14}$$

where p is a positive number. In this case, we use $p = 2$. p generally indicates the amount of emphasis that is placed on minimizing the objective function with the highest value. When $p = 1$, (14) reduces to an objective sum, and when $p = \infty$, (14) reduces to the min-max method. This approach always yields Pareto-optimal solutions.

V. Single-objective Optimization Results

In this section, numerical and visual results are presented with each performance measure used independently. These results correspond to Santos's posture when he touches the two target points shown in Figure 6.

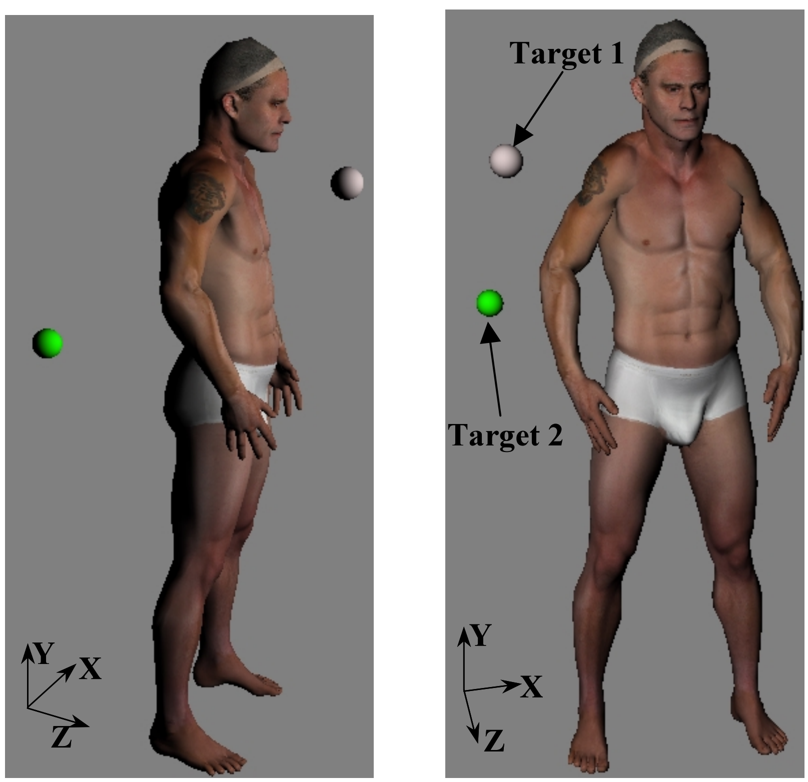

Figure 6. Target Points.

The lighter colored sphere is target 1, and the darker sphere is target 2. Target 1 is located at $(-38, 39, 34)$, and target 2 is located at $(-36, 6, -26)$. The point $(0,0,0)$ is located at Santos's hip.

In anticipation of using multi-objective optimization, the objective functions are normalized such that they all have values between zero and one. In this way, no single objective function dominates the aggregate functions used for MOO. The normalized objectives are also used for single-objective optimization, so the single-objective results are comparable to those obtained with MOO. The feasible space for the problem in (11) is variable, depending on where the target point is located. Consequently, the absolute maximum and minimum, considering all possible target points, are used for normalization. Each objective function has an absolute minimum of zero, achieved when Santos is postured in the neutral position. Therefore, each objective function is normalized simply by dividing by its corresponding maximum. The maximum values for joint displacement, discomfort, and delta-potential-energy are 287.703, 221.120, and 759.739, respectively.

The values for the normalized objective functions are given for target 1 and target 2, in Tables 3 and 4, respectively.

Table 3: Objective Function Values for Target 1

	Joint Displacement Values	Discomfort Values	Delta-Potential-Energy Values
Minimized Displacement	0.0069	0.172	0.0205
Minimize Discomfort	0.0608	0.0018	0.0252
Minimize Delta-Potential-Energy	0.6109	0.5387	0.0144

Table 4: Objective Function Values for Target 2

	Joint Displacement Values	Discomfort Values	Delta-Potential-Energy Values
Minimized Displacement	0.0096	0.1634	0.0164
Minimize Discomfort	0.0425	0.0018	0.0517
Minimize Delta-Potential-Energy	0.0365	0.3969	0.0025

Each column of these tables represents values for a particular objective function. Each row represents the design point $\mathbf{q}^*$ when a particular objective is minimized. For instance, the first value in the first column represents the minimum value for joint displacement. The second value in the first column represents the value of the displacement function evaluated at the point that minimizes discomfort. The values in Tables 3 and 4 are rather small. This is a consequence of the target points that are used in this study; other target points result in higher objective-function values. Note that the absolute values for the objective functions are not necessarily significant in terms of quantifying the concepts that each performance measure represents. Rather, we are concerned with the change in objective-function values as different postures are assumed.

For the given target points, none of the optimum points $\mathbf{q}^*$ are *dominated*, which means there is no row for which all of the values in that row are greater than the corresponding values in another row. These are conflicting objectives in that what reduces one function, increases at least one other function. Discomfort has particularly high values when delta-potential-energy is minimized. This is because, as we will show, the energy performance measure results in substantial torso movement, whereas the discomfort function incorporates the idea that such torso movement tends to be more uncomfortable than arm movement.

The postures determined when each of the objectives is minimized, are shown in Figures 7 through 9. Clearly, using different human performance measures as objectives provides significantly different results. In fact, although all of these performance measures result in postures that tend to gravitate towards the neutral position, each has its own set of advantages and potential applications.

The joint displacement function provides a fundamental objective that yields reasonable results. It provides benchmark postures that are acceptable visually. However, it often results in postures with the arm relatively close to the torso. In addition, there can be slightly more movement in the spine than one might anticipate.

The discomfort function corrects these issues. As discussed earlier, with the discomfort function, the spine only bends if necessary, and this results in postures that are more realistic especially when the target points are in front of the avatar. In essence, the discomfort function provides an accurate approximation of the lexicographic approach to multi-objective optimization. It also tends to avoid postures where the elbow hugs the torso. This tendency results from the penalty associated with joints that are near their limits, and it is noted in Figures 7 and 8 when comparing the postures with respect to target 1. When the discomfort function is used with target 2, it may appear as if the resulting posture is less natural than the posture achieved with the displacement function. However, again, this has to do with how joint limits are incorporated. Approaching the limits of a joint can result in discomfort that is not necessarily visualized.

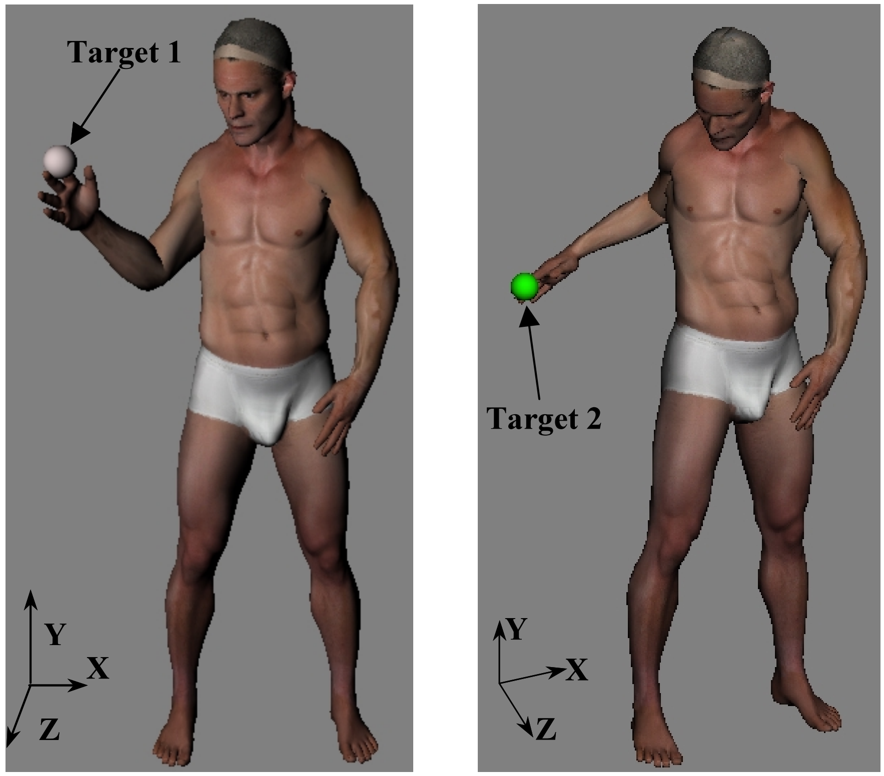

Figure 7. Postures when Joint Displacement is Minimized.

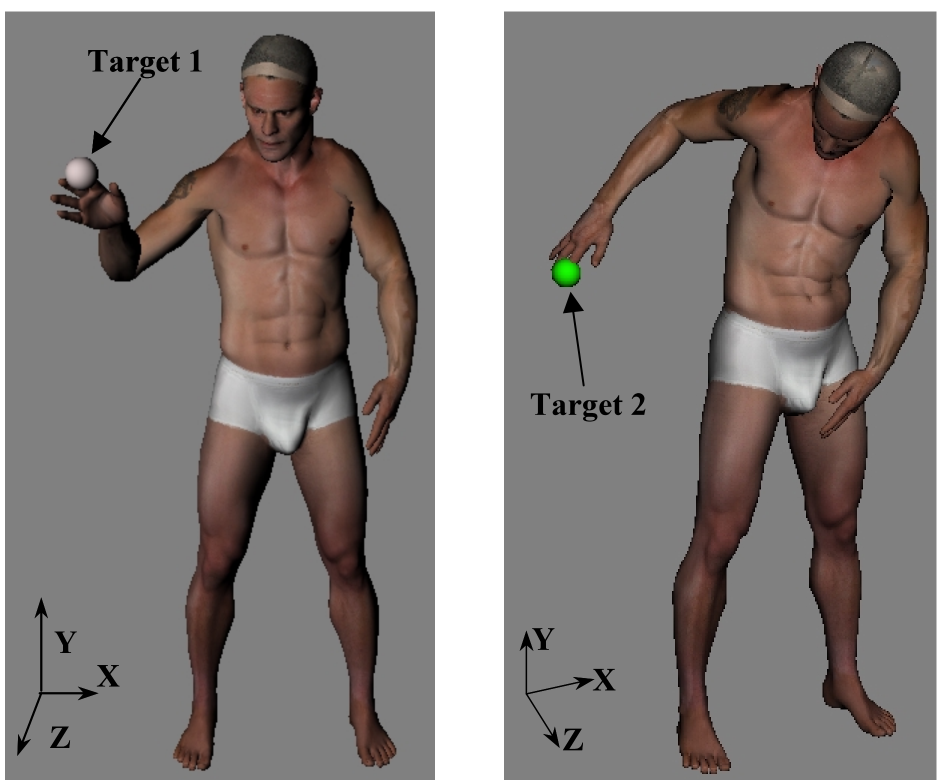

Figure 8. Postures when Discomfort is Minimized.

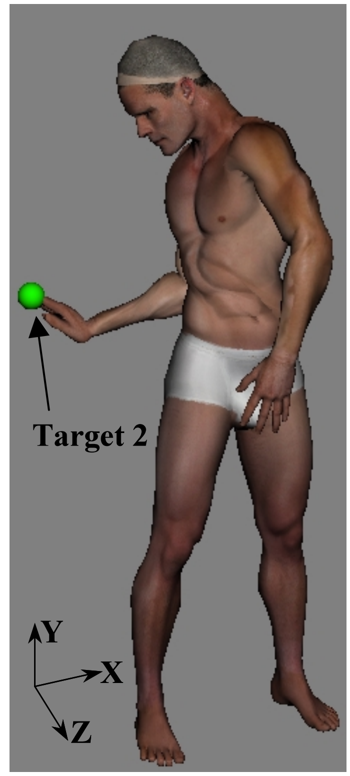

Figure 9. Postures when Delta-Potential-Energy is Minimized.

Thus, the posture determined with the displacement function, with regards to target 2, can actually be more uncomfortable than the posture predicted with the discomfort function. This discrepancy is especially true when the avatar is required to reach behind itself or across the torso.

As suggested earlier, potential energy does not change with rotation in the torso. Thus, using the delta-potential-energy performance measure independently tends to result in postures with excessive torso rotation. In addition, it can result in excessive bending in the wrist. Recall that the original hypothesis was that the mass component in potential energy would provide a natural weighting factor for the different joint values, thus alleviating the need for somewhat ad hoc weights in the joint displacement function. Although the energy function does not provide a replacement for the displacement function, it can provide useful results when coupled with other performance measures, as we will demonstrate in the next section.

VI. Multi-objective Optimization Results

The characteristics of the different performance measures are combined using MOO. As suggested earlier, we study three MOO methods: the objective sum method in (3), the min-max method in (13), and the global criterion method in (14). The objective-function values when each of these methods is used are shown in Tables 5 and 6.

Table 5: Objective Function Values for Target 1

	Joint Displacement Values	Discomfort Values	Delta-Potential-Energy Values
Objective Sum Method	0.0103	0.0019	0.0194
Global Criterion Method	0.0108	0.0032	0.0185
Min-max Method	0.0165	0.0165	0.0165

Table 6: Objective Function Values for Target 2

	Joint Displacement Values	Discomfort Values	Delta-Potential-Energy Values
Objective Sum Method	0.0148	0.0021	0.0055
Global Criterion Method	0.0132	0.0031	0.0067
Min-max Method	0.0115	0.0115	0.0115

As with the single-objective results, none of the MOO solution points is dominated. The results for the objective sum and the global criterion are similar, which is common with many MOO problems. When the min-max method is used, however, all of the objective functions have the same value. This is because all of the function constraints are active at the solution point. In general, the min-max method prevents any single objective function from becoming significantly larger than the other functions. The postures corresponding to Tables 5 and 6 are shown in Figures 10 through 12.

Compared to the postures with target 1 provided with the objective sum method and the global criterion method, the results with the min-max method indicate a slight increase in torso bending. In turn, this results in an increase in the discomfort, as shown in Table 5. With target 2, the min-max method results in less bending of the wrist. With the objective sum method and the global criterion method, excessive bending in the wrist is a result of the contribution of the delta-potential-energy function.

Using MOO (as apposed to single-objective optimization) clearly makes a difference in the final postures. It acts to balance the unique results of the independent performance measures. However, the final posture is not particularly sensitive to the MOO method that is used. The computational performance, in terms of CPU time and the number of function calls in the optimization algorithm, was similar for each of these methods.

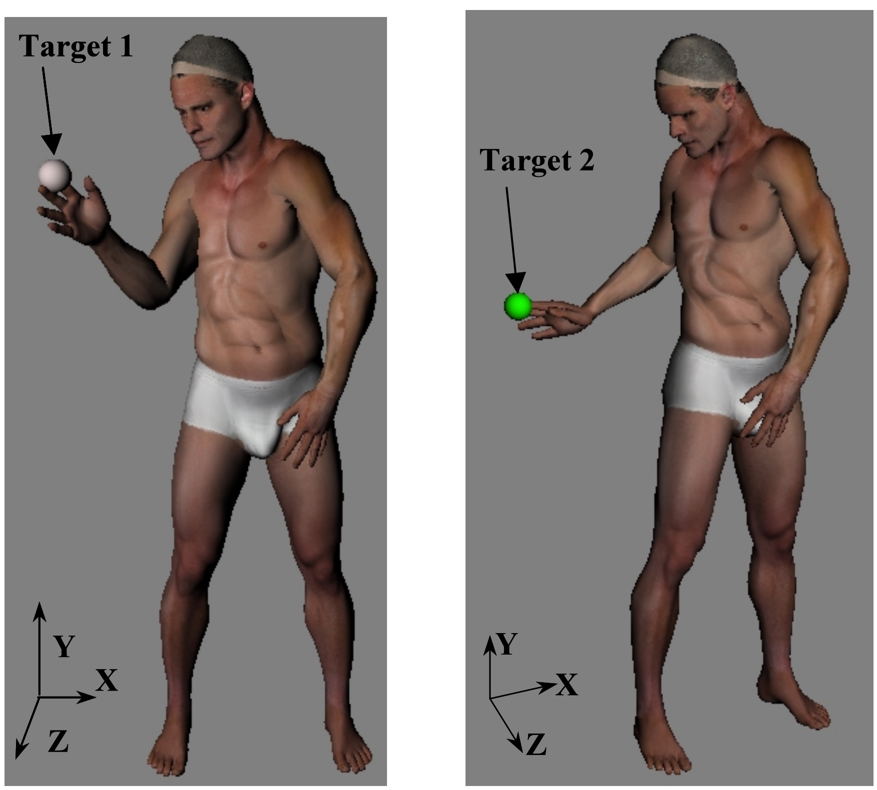

Figure 10. Postures with Objective Sum Method.

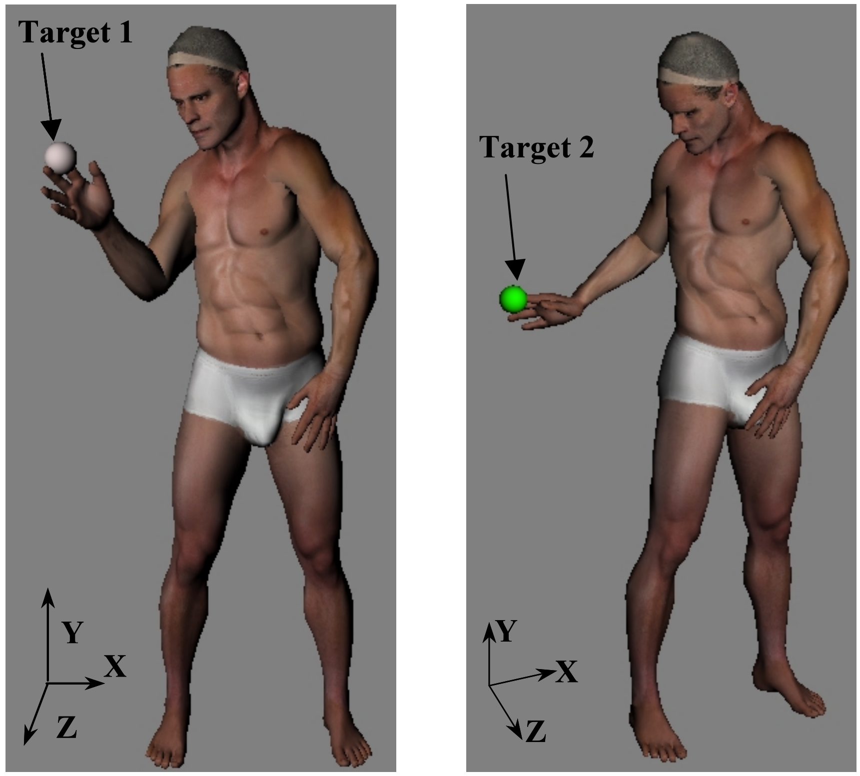

Figure 11. Postures with Global Criterion Method.

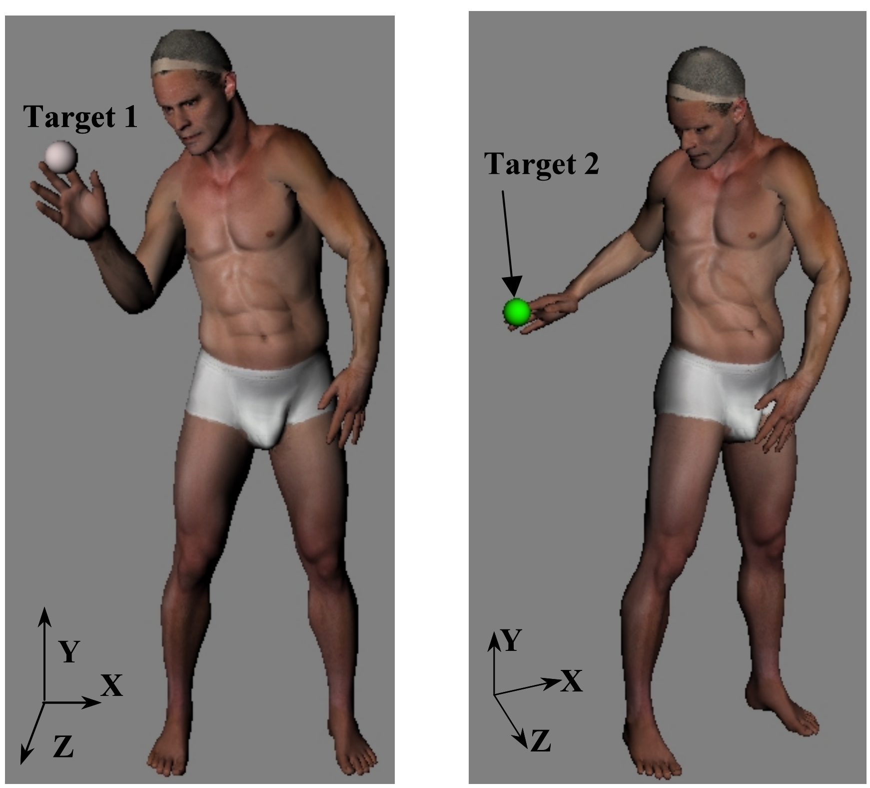

Figure 12. Postures with Min-max Method.

VII. Conclusion

A general mathematical formulation for predicting human postures has been presented, demonstrated, and augmented with the use of MOO. MOO has been used to develop new human performance measures and to aggregate these measures in an optimization-based posture prediction problem. The virtual human, Santos, has been used to evaluate different performance measures and to test the applicability of MOO to posture prediction. Each performance measure is based on a unique premise, and each is most applicable to subtly different scenarios. Which performance measure is most appropriate can depend on where a particular task is being completed relative to the avatar. Joint displacement provides a reliable standard. The discomfort function takes into consideration the discomfort of having to move one's torso and/or clavicle, and the discomfort associated with operating at the limits of one's range of motion. It provides the most realistic posture when target 1 is used. Delta-potential-energy incorporates difficulty associated with supporting the weight of different body parts. However, it allows for excessive torso rotation, and it is most appropriately used in conjunction with other performance measures.

Different MOO methods have been compared for use with optimization-based posture prediction, and although the differences in results obtained with different MOO methods are subtle, MOO in general provides consistently reasonable postures. It is particularly well suited for target points located behind the avatar. In fact, the most realistic posture with target 2 is provided with the min-max method for MOO.

In this study, we presented results for only two target points, although other targets have been tested. In general, targets requiring significant extension result in similar postures regardless of the performance measure that is used. This is because the primary difficulty with such problems is determining a feasible solution (one in which the avatar actually contacts the target point). Consequently, there are fewer feasible solutions in terms of potential postures. Targets behind the avatar depend on vision, as well as displacement, discomfort, or energy. One typically moves in order to see the target as well as to touch it. This is why one may expect substantial twist in the torso for targets behind the avatar, although such movement may actually be uncomfortable, as suggested in Figure 8. Thus, it is necessary to develop a performance measure that considers this, and such work is currently being pursued.

Postures in general depend heavily on the range of motion for each joint, and such data varies widely from person to person. We have provided a formulation that incorporates these joint limits. In addition, the new discomfort objective incorporates the discomfort associated exercising one's joints near their limits.

Acknowledgements

This research was funded by the US Army TACOM project: Digital Humans and Virtual Reality for Future Combat Systems (FCS).

References

Abdel-Malek, K., Yang, J., Brand, R., and Tanbour, E., 2001a, "Towards Understanding the Workspace of The Upper Extremities," *SAE Transactions-Journal of Passenger Cars: Mechanical Systems*, Vol. 110, Section 6, pages 2198-2206.

Abdel-Malek, K., Yu, W., and Jaber, M., 2001b, "Realistic Posture Prediction," *2001 SAE Digital Human Modeling and Simulation*.

Abdel-Malek, K., Yu, W., Mi, Z., Tanbour, E., and Jaber, M., 2001c, "Posture Prediction versus Inverse Kinematics," *Proceedings of the ASME Design Engineering Technical Conference*.

Arora, J. S., 2004, *Introduction to Optimal Design*, 2nd ed., Elsevier, San Diego, CA.

Beck, D.J. and Chaffin, D.B., 1992, "An evaluation of inverse kinematics models for posture prediction", *Computer Applications in Ergonomics, Occupational Safety and Health*, Elsevier, Amsterdam, The Netherlands, pp. 329-336.

Das, B. and Behara, D.N., 1998, "Three-dimensional workspace for industrial workstations", *Human Factors*, Vol. 40, No. 4, pp. 633-646.

Das, B. and Sengupta, A.K., 1995, "Computer-aided human modeling programs for workstation design", *Ergonomics*, Vol. 38, pp. 1958-1972.

Denavit, J. and Hartenberg, R.S., 1955, "A kinematic notation for lower-pair mechanisms based on matrices", *Journal of Applied Mechanics*, Vol. 77, pp. 215-221.

Faraway, J.J., Zhang, X.D. and Chaffin, D.B., 1999, "Rectifying postures reconstructed from joint angles to meet constraints", *Journal of Biomechanics*, Vol. 32, pp. 733-736.

Farrell, K., and Marler, R.T., 2004, "Optimization-Based Kinematic Models for Human Posture", University of Iowa, Virtual Soldier Research Program, Technical Report Number VSR-04.07.

Gill, P., Murray, W., and Saunders, A, 2002, "SNOPT: An SQP Algorithm for Large-Scale Constrained Optimization", *SIAM Journal of Optimization*, Vol. 12, No. 4, pp. 979-1006.

Jung, E.S. and Choe, J., 1996, "Human reach posture prediction based on psychophysical discomfort", *International Journal of Industrial Ergonomics*, Vol. 18, pp. 173-179.

Jung, E.S., Kee, D. and Chung, M.K., 1992, "Reach posture prediction of upper limb for ergonomic workspace evaluation**",** *Proceedings of the 36th Annual Meeting of the Human Factors Society*, Atlanta, GA, Part 1, Vol. 1, pp. 702-706.

Jung, E.S., Kee, D. and Chung, M.K., 1995, "Upper body reach posture prediction for ergonomic evaluation models", *International Journal of Industrial Ergonomics,* Vol. 16, pp. 95-107.

Kee, D., Jung, E.S., and Chang, S., 1994, "A man-machine interface model for ergonomic design", *Computers & Industrial Engineering*, Vol. 27, pp. 365-368.

Lin, C.S., Chang, P.R. and Luh, J.Y.S., 1983, "Formulation and Optimization of Cubic Polynomial Joint Trajectories for Industrial Robots", *IEEE Trans. Automat. Contr. Vol.* 28, pp. 1066–1073.

Marler, R.T., 2004, "Development of an Orientation Constraint for Human Posture Prediction Models", University of Iowa, Virtual Soldier Research Program, Technical Report Number VSR-04.11.

Marler, R.T., and Arora, J.S., 2004, "Survey of Multi-objective Optimization Methods for Engineering", *Structural and Multidisciplinary Optimization*, Vol. 26, pp. 369-395.

Mi, Z., Yang, J., Abdel-Malek, K., 2002, "Real-Time Inverse Kinematics for Humans," *Proceedings of 2002 ASME Design Engineering Technical Conferences*, DETC2002/MECH-34239, September 29-October 2, Montreal, Canada.

Miettinen, K., 1999, *Nonlinear Multiobjective Optimization*, Kluwer Academic Publishers, Boston.

Porter, J.M., Case, K., and Bonney, M.C., 1990, "Computer workspace modeling", in: J. R. Wilson and E. N. Corlett (Eds.), *Evaluation of Human Work*, Taylor & Francis, London, UK, pp. 472-499.

Romero, C., 2000, "Bi-criteria Utility Functions: Analytical Considerations and Implications in The Short-run Labor Market", *European Journal of Operations Research*, Vol. 122, No. 1, pp. 91-100.

Saramago, S.F.P. and Steffen Jr, V., "Optimization of the Trajectory Planning of Robot Manipulators taking into account the Dynamics of the System", *Mechanism and Machine Theory* 33(7), 883–894 (1998).

Saramago, S.F.P. and Steffen Jr, V., "Optimal Trajectory Planning of Robot Manipulators in the Presence of Moving Obstacles", *Mechanism and Machine Theory* 35(8), 1079–1094 (2000).

Saramago, S.F.P. and Ceccarelli, M., "An Optimum Robot Path Planning with Payload Constraints", *Robotica* 20(4), 395-404 (2002).

Shin, K.G. and Mckay, N.D., 1986, "A Dynamic Programming Approach to Trajectory Planning of Robotic Manipulators", *IEEE Trans. Automat. Contr*., Vol. AC-31(6), pp. 491–500.

Tolani, D., Goswami, A. and Badler, N., 2000, "Real-Time Inverse Kinematics Techniques for Anthropomorphic Limbs", *Graphical Models,* Vol. 62, No. 5, pp. 353-388.

Wang, X.G., 1999, "A behavior-based inverse kinematics algorithm to predict arm prehension postures for computer-aided ergonomic evaluation", *Journal of Biomechanics*, Vol. 32, pp. 453-460.

Yang, J., Abdel-Malek, K., and Nebel, K., 2003, "The Reach Envelope of a 9 Degree of Freedom Model of the Upper Extremity," (submitted) *International Journal of Robotics and Automation.*

Zhang, X. and Chaffin, D.B., 1996, "Task effects on three-dimensional dynamic postures during seated reaching movements: an analysis method and illustration", *Proceedings of the 1996 40th Annual Meeting of the Human Factors and Ergonomics Society*, Philadelphia, PA, Part 1, Vol. 1, pp. 594-598.

Zhao, J. and Bai, S.X., 1999, "Load distribution and joint trajectory planning of coordinated manipulation for two redundant robots", *Mechanism and Machine Theory*, Vol. 34, pp. 1155–1170.